

# Enhancing Electron-Nuclear Resonances by Dynamical Control Switching

Sichen Xu,<sup>1</sup> Chanying Xie,<sup>1</sup> and Zhen-Yu Wang<sup>1,2,\*</sup>

<sup>1</sup>*Key Laboratory of Atomic and Subatomic Structure and Quantum Control (Ministry of Education), and School of Physics, South China Normal University, Guangzhou 510006, China*

<sup>2</sup>*Guangdong Provincial Key Laboratory of Quantum Engineering and Quantum Materials, and Guangdong-Hong Kong Joint Laboratory of Quantum Matter, South China Normal University, Guangzhou 510006, China*

We present a general method to realize resonant coupling between spins even though their energies are of different scales. Applying the method to the electron and nuclear spin systems such as a nitrogen-vacancy (NV) center with its nearby nuclei, we show that a specific dynamical switching of the electron spin Rabi frequency achieves efficient electron-nuclear coupling, providing a much stronger quantum sensing signal and dynamic nuclear polarization than previous methods. This protocol has applications in high-field nanoscale nuclear magnetic resonances as well as low-power quantum control of nuclear spins.

## I. INTRODUCTION

Resonant coupling of spins is a common requirement in spin-based quantum technologies. A notable platform is the nitrogen-vacancy (NV) center in diamond [1–3], where the NV electron spin is used to detect, polarize, and control spins in its vicinity [4–10]. Flip-flop dynamics occur when the coupled spins have the same energy, e.g., due to the same gyromagnetic ratio of the spins [see Fig. 1(a)].

Coupling of nuclear and electron spins is of particular interests. Electron and nuclear spins usually have quite different energies, which prohibits their exchange of spin polarization. A dynamical decoupling (DD)  $\pi$  pulse sequence [6, 11–18] can induce electron-nuclear resonance for quantum information processing [4, 19–21], nano-scale nuclear magnetic resonance (NMR) [17], quantum sensing [5, 22], and dynamic nuclear polarization (DNP) [23–27]. These DD sequences in the ideal case require unbounded bang-bang control but in realistic situations the amplitude of control is bounded, where the latter can lead to spurious resonances between electron and nuclear spins [28–33]. An alternative scheme is a continuous driving on the electron spin using a bounded control amplitude, which results in a dressed electron spin where the energy splitting in the dressed basis equals the Rabi frequency of the driving [8, 34, 35]. When this Rabi frequency matches the Larmor frequency of the nuclear spin, i.e., under the Hartmann-Hahn condition [36] similar to the case in Fig. 1(a), the electron and nuclear spins have resonant coupling.

However, due to the own property of the systems we choose or some technical limits, sometimes the frequencies between the electron and nuclear spins have a large mismatch such that the Hartmann-Hahn condition can not be reached by the Rabi frequency [see Fig. 1(b)]. For instance, under a high magnetic field which would be favorable to enhance nuclear spin polarization, to pro-

long spin coherence times, or to induce large chemical shifts for nano-scale nuclear magnetic resonance (NMR), the nuclear spin Larmor frequencies can be much larger than the available Rabi frequency of the electron spin. In some applications such as those in biological environments [37], the maximal control field is restricted to avoid strong microwave heating effects that could destroy the samples [38].

In this work, we show that uneven dynamical modulation of the energies can lead to resonant coupling even when the values of the energies of the spins have large mismatch values. Our dynamical control switching (DCS) scheme provides more efficient electron-nuclear spin coupling than recent low-power control protocols [39, 40]. We demonstrate the superior performance of our protocol in quantum control and sensing of single nuclear spins.

## II. DYNAMICAL SWITCHING OF ENERGIES

Our theory can be generalized to selectively couple quantum systems of different energy scales. To demonstrate the principle of our protocol, for simplicity, consider two interacting spins with the Hamiltonian ( $\hbar = 1$ )

$$H_0 = H_S + H_I, \quad (1)$$

where  $H_S = \omega_e S_z + \omega_n I_z$  is the Hamiltonian for the two spins with  $I_z$  and  $S_z$  being their spin operators. The interaction  $H_I = a S_- I^+ + \text{h.c.}$ , where  $S_{\pm} = S_x \pm i S_y$  and  $I_{\pm} = I_x \pm i I_y$ , describes the flip-flop dynamics of the spins.  $a$  is the coupling constant. In the interaction picture of  $H_S$ , the Hamiltonian becomes

$$\tilde{H}_I(t) = a S_- I^+ e^{i(\omega_n - \omega_e)t} + \text{h.c.}, \quad (2)$$

if we assume that both the energies  $\omega_e$  and  $\omega_n$  are time-independent. When  $\omega_e = \omega_n$ , the two spins have resonant flip-flop dynamics with  $\tilde{H}_I = H_I$ , see Fig. 1(a). On the other hand, when the energy mismatch  $|\omega_n - \omega_e| \gg |a|$ , the effect of  $\tilde{H}_I(t)$  is negligible by the rotating-wave approximation, which corresponds to the case of Fig. 1(b).

\* zhenyu.wang@m.scnu.edu.cn

We aim to modulate the energy mismatch in time to preserve the effect of the interaction  $\tilde{H}_I$  even though the energy difference is large. For simplicity here we only introduce a time dependence on  $\omega_e = \omega_e(t)$ . To see the effect of the modulation of  $\omega_e$ , we calculate the leading-order effective Hamiltonian of  $\tilde{H}_I(t)$  by using the Magnus expansion [41, 42] for a time  $T$ ; it reads

$$\bar{H} = \frac{1}{T} \int_0^T \tilde{H}_I(t) dt, \quad (3)$$

$$= g a S_- I^+ + \text{h.c.} \quad (4)$$

The coupling factor

$$g \equiv \frac{1}{T} \int_0^T e^{i\phi(t)} dt, \quad (5)$$

and the difference of the dynamic phase

$$\phi(t) = \int_0^t [\omega_n - \omega_e(t')] dt' \quad (6)$$

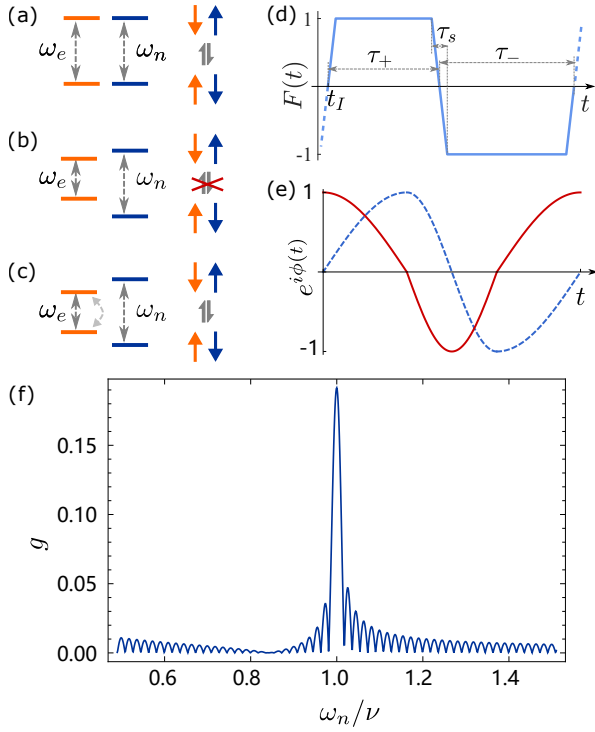


FIG. 1. (a) The spin polarization can exchange when the energies of two spins (orange and blue arrows) are the same  $\omega_e = \omega_n$ . (b) The exchange of spin polarization is prohibited when  $\omega_e \neq \omega_n$ . (c) Dynamical switching of one spin's energy as  $\omega_e = F(t)\Omega$  with  $F(t) \in \{\pm 1\}$  can induce resonant exchange of the spin polarization, even through  $|\omega_e| \ll \omega_n$ . (d)  $F(t)$  in one period  $\tau = \tau_- + \tau_+$  in which the positive control starts at  $t = t_I$ . (e) The corresponding real (red solid line) and imaginary (blue dashed line) parts of  $e^{i\phi(t)}$  under the resonance condition Eq. (12) with  $k_D = 1$ . The time integral of  $e^{i\phi(t)}$  in one period is nonzero. (f) The coupling factor  $g$  as a function of  $\omega_n/\nu$  for a total time  $T = 50\tau$ . Here  $\Omega/\nu = 0.3$  in all the plots and  $\tau_s = 0$  and  $t_I = -\frac{1}{2}\tau_+$  in (e) and (f).

can be controlled by  $\omega_e(t)$ . When  $\omega_e$  is a constant, the amplitude  $g = e^{-ix} \frac{\sin x}{x}$  decays with  $x = (\omega_e - \omega_n)T/2$  in a power-law decay manner [43]. For the resonant case  $\omega_e = \omega_n$ ,  $g = 1$ .

In this work we consider the situation that  $\omega_e$  is bounded with its maximal value  $\Omega$ , with  $|\omega_e| \leq \Omega \ll \omega_n$  and  $\omega_n - \omega_e \gg |a|$ . Because  $\omega_n - \omega_e$  is large, the integrand in Eq. (6) is a fast oscillating factor, which tends to average out the interaction. To solve the obstacle, we modulate the dynamic phase  $\phi(t)$  with uneven speed to enhance the value of  $g$  in Eq. (5). The intuition comes from the idea of uneven modulation of dynamic phases in quantum adiabatic control which has been used to accelerate quantum adiabatic process [44–47]. We assume a periodic function  $\omega_e(t) = \omega_e(t + \tau)$ , see Fig. 1(d) for an example. Let the increase of  $\phi(t)$  in one period  $\tau$  of  $\omega_e(t)$  be different from  $2k_D\pi$  (with  $k_D$  an integer) by an amount

$$\delta_\phi = \phi(\tau) - 2k_D\pi. \quad (7)$$

Using the periodicity of  $\omega_e(t)$  we calculate Eq. (5) for  $T = N\tau$ ,

$$g = \frac{1}{N\tau} \int_0^{N\tau} e^{i\phi(t)} dt = \eta J, \quad (8)$$

where the functional  $J[\phi(t)]$  is defined as

$$J[\phi(t)] = \frac{1}{\tau} \int_0^\tau e^{i\phi(t)} dt, \quad (9)$$

and the factor

$$\eta = \frac{1}{N} \sum_{m=1}^N e^{i(m-1)\delta_\phi} = e^{i\frac{N-1}{2}\delta_\phi} \frac{\sin(N\delta_\phi/2)}{N \sin(\delta_\phi/2)} \quad (10)$$

has a peak centered at  $\delta_\phi = 0$  with a width  $\sim 2\pi/N$ , see Fig. 1(f). That is, when  $\delta_\phi = 0$  the dynamic phase factors in Eq. (10) coherently add up, while for other  $\delta_\phi < \pi$ ,  $\eta \approx 0$  for a large averaging time  $T$ .

We want to maximize the functional  $J[\phi(t)]$  by using inhomogeneous changes of  $\phi(t)$ . To have a higher degree of inhomogeneity, we choose

$$\omega_e(t) = F(t)\Omega \quad (11)$$

with the periodic modulation function  $F(t) = F(t + \tau)$ . In particular, we periodically switch the value of  $\omega_e$  between the maximal value  $+\Omega$  and the minimal value  $-\Omega$ . We would like to have  $F(t) = 1$  when  $t \in [t_I, t_I + \tau_+)$  and  $F(t) = -1$  when  $t \in [t_I + \tau_+, t_I + \tau_+ + \tau_-)$  with  $\tau = \tau_+ + \tau_-$ . Our protocols starts at  $t = 0$  and therefore  $t_I$  defines the initial waveform of the control field.  $t_I = -\frac{1}{2}\tau_+$  ( $t_I = 0$ ) corresponds to a symmetric (asymmetric) control protocol. To take into account that instantaneous switching of the control field could be difficult in experiments,  $F(t)$  can have a transition time  $\tau_s$  during the switching, see Fig. 1(d). However, as we will demonstrate in the simulations of this work, as long as  $\tau_s$  is

not too large, the effect of non-zero  $\tau_s$  is negligible. For this reason, in the following theoretical analysis, we assume  $\tau_s = 0$ . We will see, using uneven durations of the positive and negative drive, i.e.,  $\tau_+ \neq \tau_-$ , can lead to stronger coupling and signal responses.

The condition for the resonance  $\delta_\phi = 0$  gives

$$\omega_n = k_D \nu + r_D (1 - k_D) \Omega, \quad (12)$$

where the ratio  $r_D = (\tau_+ - \tau_-)/\tau$  and the frequency  $\nu = 2\pi/\tau + r_D \Omega$ . Note that the resonance frequencies are different from the frequency,  $2\pi/\tau$ , of the periodic driving. Under the resonance condition Eq. (12), there is coherent coupling of spins, see Fig. 1(e). Equation (12) for  $k_D = 0$  corresponds to the resonance to a spin with  $|\omega_n| = |r_D \Omega| < \Omega$ , which is not our target of control. When  $k_D = 1$  we achieve a spin-spin resonance at  $\omega_n = \nu$ , which can be much larger than  $\Omega$ .

Under the resonance condition Eq. (12) the strength  $|J|$  has a large value, which is invariant with respect to  $t_I$  because  $t_I$  only changes the phase factor of  $J$ . For the case of symmetric control which has  $t_I = -\frac{1}{2}\tau_+$ , we obtain

$$J = 4(-1)^{k_D} \Omega \sin\left[\frac{1}{4}(1 + r_D)(\omega_n - \Omega)\tau\right] / [(\omega_n^2 - \Omega^2)\tau]. \quad (13)$$

One can maximize the signal for  $k_D \neq 0$  by maximization of  $J$ . On this regard we choose  $r_D = \Omega/\nu$ , which implies  $\tau_\pm = \pi/(\nu \mp \Omega)$  and  $g = (2\Omega)/(\pi\nu)$  when  $k_D = 1$ .

### III. LOW-POWER QUANTUM SENSING OF NUCLEAR SPINS AND DNP

We apply our method to an NV center with its surrounding nuclear spins, which is relevant to quantum information processing, quantum sensing, and nano-scale NMR, and nuclear hyperpolarization. The Hamiltonian of an NV center electronic spin and its nearby nuclear spins under a strong magnetic field  $-B_z$  along the NV symmetry axis reads  $H' = DS_z^2 + \gamma_e B_z S_z + \sum_j \gamma_j B_z I_z + S_z \sum_j (A_j^x I_j^x + A_j^z I_j^z) + H'_c$ , where  $D = (2\pi) \times 2.87$  GHz is the NV zero-field splitting,  $S_z = |1\rangle\langle 1| - |-1\rangle\langle -1| + 0|0\rangle\langle 0|$  for the NV electron spin,  $I_j^\alpha$  ( $\alpha = x, y, z$ ) are the spin operators for the  $j$ -th nucleus, and  $\gamma_e$  and  $\gamma_j$  are the gyromagnetic ratios for the NV electron and the nuclear spins, respectively. The components of the hyperfine coupling  $A_j^x$  and  $A_j^z$  are much smaller than  $\gamma_j B_z$  because of the strong magnetic field  $B_z$ . A microwave control field with a frequency  $\omega_{\text{mw}}$  applied on the NV center realizes the control Hamiltonian  $H_c = \sqrt{2}\Omega F(t) \cos(\omega_{\text{mw}}t) S_x$ , where  $\Omega F(t)$  is the Rabi frequency of the control field with  $F(t)$  being the modulation illustrated in Fig. 1(d).

To select two NV electron spin levels  $m_s = 0$  and, say,  $m_s = 1$  to form an NV qubit, we set the microwave frequency to the energy splitting between the qubit levels. In this manner, we neglect the state  $|-1\rangle$  because there is no transition to it. Moving to a rotating frame with

respect to  $H_0 = DS_z^2 + \gamma_e B_z S_z$ , we get the new Hamiltonian

$$H = \sum_j \gamma_j B_z I_z + |1\rangle\langle 1| \sum_j (A_j^x I_j^x + A_j^z I_j^z) + H_c, \quad (14)$$

where  $H_c = F(t) \frac{\Omega}{2} (|1\rangle\langle 0| + \text{H.c.})$ . Then, with  $|+\rangle = \frac{1}{\sqrt{2}}(|1\rangle + |0\rangle)$ ,  $|-\rangle = \frac{1}{\sqrt{2}}(|1\rangle - |0\rangle)$ , the Pauli operators  $\sigma_z = |1\rangle\langle 0| + |0\rangle\langle 1| = |+\rangle\langle +| - |-\rangle\langle -|$  and  $\sigma_x = |+\rangle\langle -| + |-\rangle\langle +|$ , and the identity operator  $I = |1\rangle\langle 1| + |0\rangle\langle 0|$  for the NV electron qubit, Eq. (14) can be written as

$$H = \omega_e(t) \frac{\sigma_z}{2} + \sum_j \omega_{n,j} I_j^z + H_I, \quad (15)$$

where the qubit energy splitting  $\omega_e(t) = \Omega F(t)$  is bounded with the maximal absolute value  $\Omega$  because of experimental limitation, and the nuclear spin frequency  $\omega_{n,j} = \gamma_j B_z + \frac{1}{2} A_{z,j}$  for the  $j$ th spin is shifted by the hyperfine component  $A_{z,j}$ , which is different for different nuclear spins because the electron-nuclear coupling is position dependent. Here the electron-nuclear interaction  $H_I = \frac{1}{2} \sigma_x \sum_j (A_j^x I_j^x + A_j^z I_j^z)$  in the rotating frame

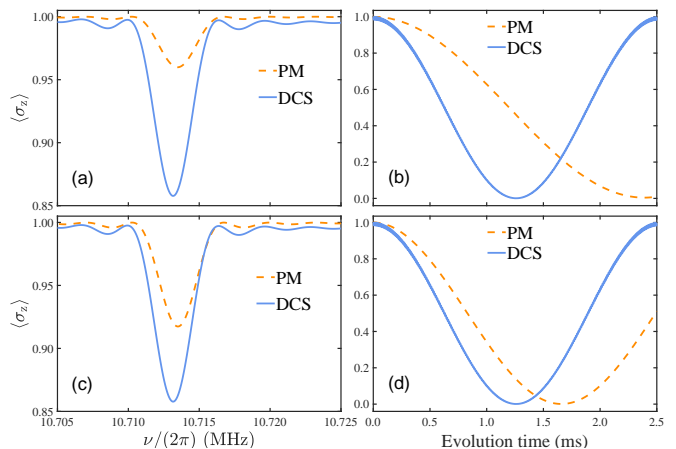


FIG. 2. Polarization signals  $\langle \sigma_z \rangle$  obtained by using our DCS (blue solid line) and those obtained by the phase modulation (PM) protocol proposed in Refs. [39, 40] (orange dashed line). (a) Spectral response of the signal. The Rabi frequency of our protocol is  $\Omega = 2\pi \times 1$  MHz. The Rabi frequency for the PM protocol is  $\Omega_0 + e^{i\theta'} \Omega_1$ , where  $\theta'$  is periodically modulated with the values 0 and  $\pi$  with an interval of  $\tau/2$ ; and we choose the typical values of  $\Omega_0 = \Omega_1 = 2\pi \times 0.5$  MHz as in Ref. [39]. Both protocols have the same maximal Rabi frequency. For comparison the sensing time  $T = 0.308$  ms is also the same for both protocols. (b) The signal as a function of the total sensing time  $T$  when the frequency  $\nu$  is set to the resonance point in (a). (c) [(d)] As (a) [(b)]. In (c) and (d)  $\Omega_0 = \Omega_1 \approx (1/\sqrt{2})\Omega$  for the PM protocol such that its average power [39] is the same as our protocol.  $t_I = -\frac{1}{2}\tau_+$  and  $\tau_s = 0$  for all plots. The protocol proposed in this work provides stronger sensing signals than previous methods.

of  $\omega_e(t)\frac{\sigma_z}{2} + \sum_j \omega_{n,j} I_j^z$  becomes

$$\begin{aligned} \tilde{H}_I(t) = & \sum_j \frac{1}{4} A_j^z I_j^z (\sigma_+ e^{i \int_0^t \omega_e dt'} + \text{h.c.}) \\ & + \sum_j \frac{1}{4} A_j^x (\sigma_+ I_j^- e^{i \int_0^t (\omega_e - \omega_{n,j}) dt'} + \text{h.c.}) \\ & + \sum_j \frac{1}{4} A_j^x (\sigma_+ I_j^+ e^{i \int_0^t (\omega_e + \omega_{n,j}) dt'} + \text{h.c.}), \end{aligned} \quad (16)$$

where  $\sigma_{\pm} = \frac{1}{2}(\sigma_x \pm i\sigma_y)$  and  $I_j^{\pm} = I_j^x \pm iI_j^y$ .

We consider the regime that the nuclear Zeeman energies  $\gamma_j B_z$  is much larger than the Rabi frequency  $\Omega$  reachable in experiments, e.g., due to the low power of the microwave field at the NV center and the strong magnetic field  $B_z$ . For this situation, the Hartmann-Hahn condition can not be met for electron-nuclear coupling, see Fig. 1(b). However, according to the resonance condition Eq. (12) for the dynamic phase Eq. (6), the coupling is preserved if the frequencies of the nuclear spin meet the resonance condition. For example, if only one nuclear spin (say,  $j = 1$ ) meets the resonance condition, we

can approximate the interaction by the effective Hamiltonian in the leading-order (say, by using the Magnus expansion)

$$\tilde{H}_I \approx \frac{\Omega}{2\pi\nu} A_1^x \sigma_+ I_1^- + \text{h.c.}, \quad (17)$$

when  $\omega_{n,1} = \nu$  or

$$\tilde{H}_I \approx \frac{\Omega}{2\pi\nu} A_1^x \sigma_+ I_1^+ + \text{h.c.}, \quad (18)$$

when  $\omega_{n,1} = \nu - 2\Omega^2/\nu$ . Equation (17) or (18) can be used to detect and control single nuclear spins, e.g., for two-qubit gates between the NV and only one nucleus.

To demonstrate the superior performance of our DCS method in low-power control, we perform numerical simulations for an NV center and a weakly coupled  $^{13}\text{C}$  nucleus with  $A_1^x = 2\pi \times 13.42$  kHz and  $A_1^z = 2\pi \times 17.09$  kHz. A strong magnetic field  $B_z = 1$  T gives a strong Zeeman energy  $\approx 2\pi \times 11$  MHz for the  $^{13}\text{C}$  nuclear spin, which is much larger than the Rabi frequency of the NV electron spin in our simulations. In the simulations, we assume that before the protocol the initial state of  $^{13}\text{C}$  nuclear spin is in a thermal state  $\rho_n \approx I/2$  and the NV electron spin is initially prepared in the eigenstate  $|+\rangle$  of  $\sigma_z$ . After a time  $T$  of the control, the density matrix of the electron and nuclear spins becomes  $\rho(T)$ . As shown in Fig. 2, the polarization  $\langle \sigma_z \rangle = \text{Tr}[\rho(T)\sigma_z]$  of the NV electron spin changes significantly at the resonance peak of  $\nu = \omega_n \approx 2\pi \times 10.713$  MHz, transferring the electron spin polarization to the nuclear spin. At  $\nu = \omega_n$  the signal  $\langle \sigma_z \rangle = \cos^2(\frac{\Omega}{2\pi\nu} A_1^x T)$ . The realized electron-nuclear coupling is more stronger than the previous protocol proposed in Refs. [39, 40], as shown in Fig. 2.

We note that our DCS protocol also provides a significant enhancement for DNP. To demonstrate its superior performance, we compare DCS with the time-optimized pulsed dynamic nuclear polarization (TOP-DNP) protocol recently developed in [26], which was shown to perform much better than the traditional nuclear spin orientation via electron spin locking (NOVEL) [26]. A

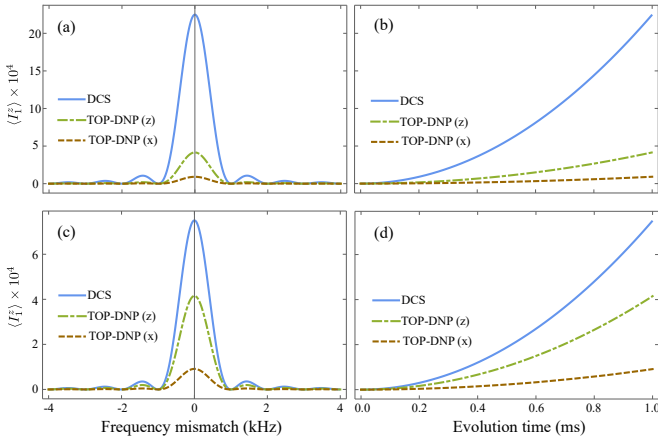


FIG. 3. Application to DNP. (a) Blue solid line is the nuclear polarization after the control of our DCS protocol for a total time  $T \approx 1$  ms, when the nuclear spin is in a high temperature thermal state. The green dash-dotted (brown dashed) line is the result when one uses the TOP-DNP protocol with the initial electron spin state initialized to be parallel (to be perpendicular) to the direction of the magnetic field of 0.35 T along the  $z$  axis, using the optimized parameters such that the microwave pulses have a length  $\tau_p = 56$  ns and a tunable frequency detuning and are separated by a delay  $d = 28$  ns (see [26]). Both protocols have the same maximal value of the Rabi frequency  $2\pi \times 2$  MHz. (b) The signal as a function of the total polarization time  $T$  when the frequency mismatch vanishes in (a), that is, when  $\nu = \omega_n$  for the DCS protocol and  $\omega_m + \omega_{\text{eff}} = \omega_n$ , where  $\omega_m = 2\pi/(\tau_p + d)$  and  $\omega_{\text{eff}}$  is the effective field [26] for the TOP-DNP protocol. (c) [(d)] As (a) [(b)], but with a reduced Rabi frequency of the DCS protocol, ensuring both DCS and TOP-DNP have the same average power. DCS provides much higher nuclear polarization. Here  $\tau_s = 0$  and  $t_I = -\frac{1}{2}\tau_+$  for DCS.

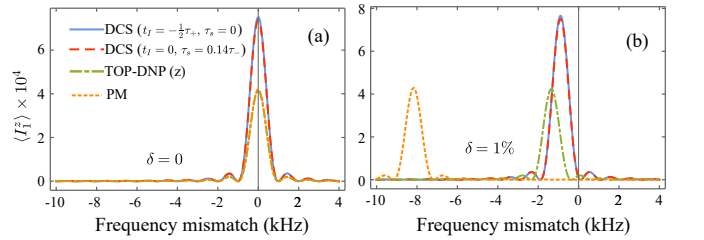


FIG. 4. Robustness of the DCS, PM, and TOP-DNP protocols. (a) The nuclear polarization obtained by the protocols without control errors, using the same parameters in Fig. 3(c). The PM protocol has the same average power as other protocols. The result of DCS with non-instantaneous switching ( $\tau_s = 0.14\tau_-$ ) and a different  $t_I$  is also shown by a red dashed line. (b) As (a), but by adding a relative error  $\delta = 1\%$  to the amplitude of the control field.

TOP-DNP sequence is composed of a train of microwave pulses of a length  $\tau_p$  separated by a delay  $d$  between the pulses [26]. In Fig. 3 we consider the polarization of a  $^1\text{H}$  spin using an electron spin. The  $^1\text{H}$  spin with  $A_1^x = 2\pi \times 0.5$  kHz and  $A_1^z = 2\pi \times 0.5$  kHz under a magnetic field 0.35 T has a Larmor frequency  $\omega_n/(2\pi) \approx 14.9$  MHz much larger than the Rabi frequency. We use the optimized parameters of TOP-DNP in [26]. As shown in Fig. 3 our DCS still gives a much higher nuclear spin polarization than the high-performance TOP-DNP protocol.

We further compare DCS, PM, and TOP-DNP protocols in Fig. 4, where we can see that the DCS protocol gives the same signal response for different values of  $t_I$  and when  $\tau_s$  is not too large. The signal strengths of the PM and TOP-DNP protocols are similar and much weaker than that of DCS. We compare the protocols when the control field has an error such that the Rabi frequency is changed from the ideal one  $\Omega(t)$  to  $(1+\delta)\Omega(t)$ . A comparison of Fig. 4(a) and (b) shows that DCS is less sensitive to this error. This robustness is a consequence of the resonance condition Eq. (12), which implies that an error  $\delta\Omega$  of the Rabi frequency only shift the resonance frequency by a smaller amount  $r_D\delta\Omega$  because  $r_D < 1$ . The factor  $r_D \ll 1$  for low-power driving  $\Omega \ll \omega_n$ .

#### IV. CONCLUSION

We have shown that uneven modulation of the dynamic phases via dynamical switching of the energy of

a quantum system, e.g., in a dressed state picture, can induce resonant response with its surrounding quantum system even through their energy scales are different. We have applied this idea to achieve low-power quantum sensing of single nuclear spins and DNP by an electron spin, even through the available electron spin Rabi frequency of the control field is much weaker than the frequencies of nuclear spins. Our results show that our protocol provides much better power efficiency and stronger sensing signals and DNP than previous power-efficient methods [26, 39, 40]. Our protocol would have useful applications in nanoscale NMR for samples that are sensitive to heating by control field, in quantum information processing with high-frequency nuclear spins, as well as other applications not specific to NV centers.

#### ACKNOWLEDGMENTS

This work was supported by National Natural Science Foundation of China (Grant No. 12074131) and the Natural Science Foundation of Guangdong Province (Grant No. 2021A1515012030).

S.X. and C.X. contributed equally to this work.

- 
- [1] M. W. Doherty, N. B. Manson, P. Delaney, F. Jelezko, J. Wrachtrup, and L. Hollenberg, The nitrogen-vacancy colour centre in diamond, *Phys. Rep.* **528**, 1 (2013).
  - [2] V. Dobrovitski, G. Fuchs, A. Falk, C. Santori, and D. Awschalom, Quantum control over single spins in diamond, *Annu. Rev. Condens. Matter Phys.* **4**, 23 (2013).
  - [3] R. Schirhagl, K. Chang, M. Loretz, and C. L. Degen, Nitrogen-vacancy centers in diamond: nanoscale sensors for physics and biology, *Annu. Rev. Phys. Chem.* **65**, 83 (2014).
  - [4] C. E. Bradley, J. Randall, M. H. Abobeih, R. C. Berrevoets, M. J. Degen, M. A. Bakker, M. Markham, D. J. Twitchen, and T. H. Taminiau, A ten-qubit solid-state spin register with quantum memory up to one minute, *Phys. Rev. X* **9**, 031045 (2019).
  - [5] C. L. Degen, F. Reinhard, and P. Cappellaro, Quantum sensing, *Rev. Mod. Phys.* **89**, 035002 (2017).
  - [6] J. Casanova, Z.-Y. Wang, J. F. Haase, and M. B. Plenio, Robust dynamical decoupling sequences for individual nuclear-spin addressing, *Phys. Rev. A* **92**, 042304 (2015).
  - [7] D. R. Glenn, D. B. Bucher, J. Lee, M. D. Lukin, H. Park, and R. L. Walsworth, High-resolution magnetic resonance spectroscopy using a solid-state spin sensor, *Nature* **555**, 351 (2018).
  - [8] J.-M. Cai, F. J., M. B. Plenio, and A. Retzker, Diamond-based single-molecule magnetic resonance spectroscopy, *New J. Phys.* **15**, 013020 (2013).
  - [9] Z.-Y. Wang, J. F. Haase, J. Casanova, and M. B. Plenio, Positioning nuclear spins in interacting clusters for quantum technologies and bioimaging, *Phys. Rev. B* **93**, 174104 (2016).
  - [10] J. Jiang and Q. Chen, Selective nuclear-spin interaction based on a dissipatively stabilized nitrogen-vacancy center, *Phys. Rev. A* **105**, 042426 (2022).
  - [11] L. Viola, E. Knill, and S. Lloyd, Dynamical decoupling of open quantum systems, *Phys. Rev. Lett.* **82**, 2417 (1999).
  - [12] Z.-Y. Wang and R.-B. Liu, Protection of quantum systems by nested dynamical decoupling, *Phys. Rev. A* **83**, 022306 (2011).
  - [13] A. M. Souza, G. A. Álvarez, and D. Suter, Robust dynamical decoupling, *Philos. Trans. R. Soc. A: Math. Phys. Eng. Sci.* **370**, 4748 (2012).
  - [14] S. Kolkowitz, Q. P. Unterreithmeier, S. D. Bennett, and M. D. Lukin, Sensing distant nuclear spins with a single electron spin, *Phys. Rev. Lett.* **109**, 137601 (2012).
  - [15] T. H. Taminiau, J. J. T. Wagenaar, T. van der Sar, F. Jelezko, V. V. Dobrovitski, and R. Hanson, Detection and control of individual nuclear spins using a weakly coupled electron spin, *Phys. Rev. Lett.* **109**, 137602 (2012).

- (2012).
- [16] N. Zhao, J. Honert, B. Schmid, M. Klas, J. Isoya, M. Markham, D. Twitchen, F. Jelezko, R.-B. Liu, H. Fedder, and J. Wrachtrup, Sensing single remote nuclear spins, *Nat. Nanotechnol.* **7**, 657 (2012).
- [17] C. Munuera-Javaloy, R. Puebla, and J. Casanova, Dynamical decoupling methods in nanoscale NMR, *Europhys. Lett.* **134**, 30001 (2021).
- [18] O. T. Whaites, J. Randall, T. H. Taminiau, and T. S. Monteiro, Adiabatic dynamical-decoupling-based control of nuclear spin registers, *Phys. Rev. Research* **4**, 013214 (2022).
- [19] J. Casanova, Z.-Y. Wang, and M. B. Plenio, Noise-resilient quantum computing with a nitrogen-vacancy center and nuclear spins, *Phys. Rev. Lett.* **117**, 130502 (2016).
- [20] B. Tratzmiller, J. F. Haase, Z. Wang, and M. B. Plenio, Parallel selective nuclear-spin addressing for fast high-fidelity quantum gates, *Phys. Rev. A* **103**, 012607 (2021).
- [21] S. Pezzagna and J. Meijer, Quantum computer based on color centers in diamond, *Appl. Phys. Rev.* **8**, 011308 (2021).
- [22] S. Nishimura, K. M. Itoh, J. Ishi-Hayase, K. Sasaki, and K. Kobayashi, Floquet engineering using pulse driving in a diamond two-level system under large-amplitude modulation, *Phys. Rev. Appl.* **18**, 064023 (2022).
- [23] V. Jacques, P. Neumann, J. Beck, M. Markham, D. Twitchen, J. Meijer, F. Kaiser, G. Balasubramanian, F. Jelezko, and J. Wrachtrup, Dynamic polarization of single nuclear spins by optical pumping of nitrogen-vacancy color centers in diamond at room temperature, *Phys. Rev. Lett.* **102**, 057403 (2009).
- [24] I. Schwartz, J. Scheuer, B. Tratzmiller, S. Müller, Q. Chen, I. Dhand, Z.-Y. Wang, C. Müller, B. Naydenov, F. Jelezko, and M. B. Plenio, Robust optical polarization of nuclear spin baths using hamiltonian engineering of nitrogen-vacancy center quantum dynamics, *Sci. Adv.* **4**, eaat8978 (2018).
- [25] J. E. Lang, D. A. Broadway, G. A. L. White, L. T. Hall, A. Stacey, L. C. L. Hollenberg, T. S. Monteiro, and J.-P. Tetienne, Quantum bath control with nuclear spin state selectivity via pulse-adjusted dynamical decoupling, *Phys. Rev. Lett.* **123**, 210401 (2019).
- [26] K. O. Tan, C. Yang, R. T. Weber, G. Mathies, and R. G. Griffin, Time-optimized pulsed dynamic nuclear polarization, *Sci. Adv.* **5**, eaav6909 (2019).
- [27] B. Corzilius, High-field dynamic nuclear polarization, *Annu. Rev. Phys. Chem.* **71** (2020).
- [28] M. Loretz, J. M. Boss, T. Rosskopf, H. J. Mamin, D. Rugar, and C. L. Degen, Spurious harmonic response of multipulse quantum sensing sequences, *Phys. Rev. X* **5**, 021009 (2015).
- [29] J. F. Haase, Z.-Y. Wang, J. Casanova, and M. B. Plenio, Pulse-phase control for spectral disambiguation in quantum sensing protocols, *Phys. Rev. A* **94**, 032322 (2016).
- [30] J. E. Lang, J. Casanova, Z.-Y. Wang, M. B. Plenio, and T. S. Monteiro, Enhanced resolution in nanoscale nmr via quantum sensing with pulses of finite duration, *Phys. Rev. Appl.* **7**, 054009 (2017).
- [31] Z. Shu, Z. Zhang, Q. Cao, P. Yang, M. B. Plenio, C. Müller, J. Lang, N. Tomek, B. Naydenov, L. P. McGuinness, F. Jelezko, and J. Cai, Unambiguous nuclear spin detection using an engineered quantum sensing sequence, *Phys. Rev. A* **96**, 051402(R) (2017).
- [32] Z.-Y. Wang, J. E. Lang, S. Schmitt, J. Lang, J. Casanova, L. McGuinness, T. S. Monteiro, F. Jelezko, and M. B. Plenio, Randomization of pulse phases for unambiguous and robust quantum sensing, *Phys. Rev. Lett.* **122**, 200403 (2019).
- [33] Z. Wang, J. Casanova, and M. B. Plenio, Enhancing the robustness of dynamical decoupling sequences with correlated random phases, *Symmetry* **12**, 730 (2020).
- [34] P. London, J. Scheuer, J.-M. Cai, I. Schwarz, A. Retzker, M. B. Plenio, M. Katagiri, T. Teraji, S. Koizumi, J. Isoya, R. Fischer, L. P. McGuinness, B. Naydenov, and F. Jelezko, Detecting and polarizing nuclear spins with double resonance on a single electron spin, *Phys. Rev. Lett.* **111**, 067601 (2013).
- [35] J.-M. Cai, B. Naydenov, R. Pfeiffer, L. P. McGuinness, K. D. Jahnke, F. Jelezko, M. B. Plenio, and A. Retzker, Robust dynamical decoupling with concatenated continuous driving, *New J. Phys.* **14**, 113023 (2012).
- [36] S. R. Hartmann and E. L. Hahn, Nuclear double resonance in the rotating frame, *Phys. Rev.* **128**, 2042 (1962).
- [37] Y. Wu, F. Jelezko, M. B. Plenio, and T. Weil, Diamond quantum devices in biology, *Angew. Chem. Int. Ed.* **55**, 6586 (2016).
- [38] Q.-Y. Cao, P.-C. Yang, M.-S. Gong, M. Yu, A. Retzker, M. B. Plenio, C. Müller, N. Tomek, B. Naydenov, L. P. McGuinness, F. Jelezko, and J.-M. Cai, Protecting quantum spin coherence of nanodiamonds in living cells, *Phys. Rev. Appl.* **13**, 024021 (2020).
- [39] J. Casanova, E. Torrontegui, M. B. Plenio, J. J. García-Ripoll, and E. Solano, Modulated continuous wave control for energy-efficient electron-nuclear spin coupling, *Phys. Rev. Lett.* **122**, 010407 (2019).
- [40] N. Aharon, I. Schwartz, and A. Retzker, Quantum control and sensing of nuclear spins by electron spins under power limitations, *Phys. Rev. Lett.* **122**, 120403 (2019).
- [41] E. S. Mananga and T. Charpentier, On the floquet-magnus expansion: Applications in solid-state nuclear magnetic resonance and physics, *Phys. Rep.* **609**, 1 (2016).
- [42] U. Haeberlen and J. S. Waugh, Coherent averaging effects in magnetic resonance, *Phys. Rev.* **175**, 453 (1968).
- [43] J. F. Haase, Z.-Y. Wang, J. Casanova, and M. B. Plenio, Soft quantum control for highly selective interactions among joint quantum systems, *Phys. Rev. Lett.* **121**, 050402 (2018).
- [44] Z.-Y. Wang and M. B. Plenio, Necessary and sufficient condition for quantum adiabatic evolution by unitary control fields, *Phys. Rev. A* **93**, 052107 (2016).
- [45] K. Xu, T. Xie, F. Shi, Z.-Y. Wang, X. Xu, P. Wang, Y. Wang, M. B. Plenio, and J. Du, Breaking the quantum adiabatic speed limit by jumping along geodesics, *Sci. Adv.* **5**, eaax3800 (2019).
- [46] W. Zheng, J. Xu, Z. Wang, Y. Dong, D. Lan, X. Tan, and Y. Yu, Accelerated quantum adiabatic transfer in superconducting qubits, *Phys. Rev. Appl.* **18**, 044014 (2022).
- [47] Y. Liu and Z.-Y. Wang, Shortcuts to adiabaticity with inherent robustness and without auxiliary control, *arXiv preprint arXiv:2211.02543* (2022).